



ARCHIVES of FOUNDRY ENGINEERING

ISSN (2299-2944)



10.24425/afe.2025.155381

Published quarterly as the organ of the Foundry Commission of the Polish Academy of Sciences

Effect of Ni Addition on the Hardness and Impact Resistance of Manganese Cast Steel for Railway Infrastructure Castings

T. Wróbel^{a, b, *} , S. Sobula^c , G. Tęcza^c , D. Bartocha^{a, b} , J. Jezierski^{a, b} , K. Kostrzewa^b^a Silesian University of Technology, Department of Foundry Engineering, Towarowa 7, 44-100 Gliwice, Poland^b Huta Małapanew Sp. z o.o., Kolejowa 1, 46-040 Ozimek, Poland^c AGH University of Science and Technology, Department of Alloys and Cast Composites Engineering, Reymonta 23, 30-059 Kraków, Poland

* Corresponding author. E-mail address: tomasz.wrobel@polsl.pl

Received 17.09.25; accepted in revised form 18.10.25; available online 22.12.2025

Abstract

This paper presents the results of research concerning manganese cast steel, also called Hadfield cast steel. The aim of the research was to determine the effect of Ni addition on the usable properties, i.e., hardness and impact resistance of manganese cast steel for cast components of railway crossovers. The scope of the research included making test castings with a unit weight of 1.5 kg in molds from molding sand prepared using Alphaset technology on a chromite sand matrix. The technological process of the test castings included heat treatment, i.e., oversaturation in water from a temperature of 1050°C. The effect of Ni addition from approx. 0,1 to approx. 1,5 wt.% on the usable properties of manganese cast steel were assessed through impact resistance tests performed in a railway impact bending test, Brinell hardness measurements, and microstructure analysis using light optical and scanning electron microscopy. Analysis of the obtained experimental results allowed for the optimization of the chemical composition of manganese cast steel for cast elements of railway infrastructure.

Keywords: Manganese cast steel, Nickel, Railway crossovers, Hardness, Impact resistance

1. Introduction

Manganese alloy cast steel was originally developed and patented by Sir Robert H. Hadfield in 1883 in the United Kingdom (patent no. 200). In recognition of the achievements of this outstanding English metallurgist, steel and cast steel containing about 1,0÷1,4 wt.% carbon and 12,0÷14,0 wt.% manganese, while maintaining the Mn:C ratio of 10, and characterized by an austenitic microstructure after the heat treatment of type oversaturation, is commonly referred to as Hadfield steel or Hadfield cast steel. According to the discovery presented in [1] in 1888, also by R. H. Hadfield, an essential feature of this Fe-based

alloy is its ability to work-harden under increased pressure or load, e.g. as a result of impact. This manifests itself in increased surface hardness and wear resistance while maintaining core ductility. Consequently, such cast steels are widely classified as abrasion-resistant alloys [2–5].

The basic alloying elements of Hadfield cast steel are C and Mn, quantitatively balanced so that after the heat treatment of type oversaturation from a temperature of 1050°C in water, a fully austenitic microstructure is obtained. The necessity of applying the heat treatment of type oversaturation in the technological process of manganese cast steel results from the need to modify its as-cast microstructure, which contains a significant amount of carbides, i.e. alloy cementite (Fe, Mn)₃C, usually located along austenite



© The Author(s) 2025. Open Access. This article is licensed under a Creative Commons Attribution 4.0 International License (<http://creativecommons.org/licenses/by/4.0/>), which permits use, sharing, adaptation, distribution and reproduction in any medium or format, as long as you give appropriate credit to the original author(s) and the source, provide a link to the Creative Commons licence, and indicate if changes were made.

grain boundaries. The heat treatment of type oversaturation with rapid cooling in water prevents diffusion transformations and thus inhibits the precipitation of carbides previously dissolved during heating in the furnace prior to quenching. The resulting high-manganese austenite already at room temperature, under heavy surface loads, shows a strong tendency to work hardening, which occurs due to mechanical twinning and strain-induced martensitic transformation [2, 6–8]. As a result, the hardened surface layer, composed of austenite with numerous microtwins and martensitic regions, exhibits significantly higher strength properties compared to the bulk of the casting. It should be emphasized that this strengthening, manifested mainly by increased surface hardness and abrasion resistance, is much more pronounced than in the case of other austenitic alloy cast steels, e.g. Cr–Ni cast steels [8].

The mechanical properties of manganese cast steel in an oversaturated state, typically fall within the following ranges: UTS = 600÷1000 MPa, YS = 350÷420 MPa, EL = 15÷20%, KCU = 100÷250 J/cm², and HB = 180÷280 [8, 9]. In conditions of work hardening, the surface hardness of manganese cast steel castings can increase several times up to HB = 500÷1000 [8, 15–17]. Since the above-mentioned strengthening is limited to

surface regions, the ductility of the casting wall is retained. The combination of high surface hardness with core ductility determines the applicability of manganese cast steel to hammers and liners for coal and other mills, cone crusher parts, construction machinery components, as well as cast railway crossover elements [8–15].

However, it should be noted that according to the literature [8, 9], in the case of thick-walled castings (wall thickness > 70 mm), achieving a fully austenitic microstructure after the heat treatment of type oversaturation is only possible with the addition of 0.5÷4.0 wt.% Ni to the chemical composition of manganese cast steel. However, due to the high cost of Ni, very important is find of optimal Ni amount for a compromise between the economics of the manufacturing process and the mechanical properties for each type of casting. Since the presented research results are dedicated to thick-walled cast railway crossover components, i.e. Insert type frogs (Fig. 1) used in welded–bolted crossovers with steel rails, and monoblock frogs (Fig. 2) used in welded crossovers with steel rails, the aim of the study was to determine the effect of Ni concentration on the impact resistance, hardness, and microstructure of Hadfield cast steel.



Fig. 1. Scheme of Insert frog R500 (R – turnout radius in meters)



Fig. 2. Scheme of monoblock frog R500 (R – turnout radius in meters)

Table 1.

Chemical composition of the studied manganese cast steel

Elements concentration, wt. %										
C	Mn	Si	Ni	Cr	Mo	Cu	Ti	Al	S	P
Variant 0										
1.10	12.10	0.45	0.10	0.27	0.08	0.01	0.047	0.014	0.015	0.035
Variant 1										
1.05	12.24	0.45	0.51	0.25	0.09	0.01	0.055	0.015	0.014	0.037
Variant 2										
1.09	12.11	0.38	0.98	0.30	0.05	0.01	0.050	0.010	0.014	0.039
Variant 3										
1.08	11.99	0.44	1.48	0.30	0.04	0.01	0.050	0.012	0.013	0.040

2. Experimental procedure

Table 1 presents the chemical composition of the studied manganese cast steel, determined using a SPEKTROMAXx optical emission spectrometer with spark excitation.

The process variable was the Ni content in the range of approx. 0,1÷1,5 wt.%. In addition, all experimental melts were modified by introducing 0,05 wt.% Ti into the liquid alloy in the form of FeTi70 ferroalloy. The experimental melts were carried out in a 30 kg capacity induction furnace, melting manganese cast steel charge material supplied by Huta Malapanew Sp. z o.o. In each case, the required amount of Ni (99.95 wt.% purity) was added to the charge, and the overheating and pouring temperatures were set to $1550 \pm 10^\circ\text{C}$ and $1460 \pm 10^\circ\text{C}$, respectively. Test castings were made in moulds prepared with chromite sand bonded with Permabind 408 resin and Permabind Plus 8 hardener. High-purity chromite sand was used, confirmed according to the quality assessment method described in [18]. Resin was added at 1,2 wt.% of sand mass, while the hardener was added at 25,0 wt.% of resin mass.

For each Ni concentration variant, three test castings (Fig. 3) with dimensions of $30 \times 30 \times 200\text{mm}$, a unit mass of 1,5kg, and a cast U-notch with a radius of 1.5mm (Fig. 4) were made in one mould. After knockout and cleaning, all test castings underwent heat treatment by water oversaturation from 1050°C .

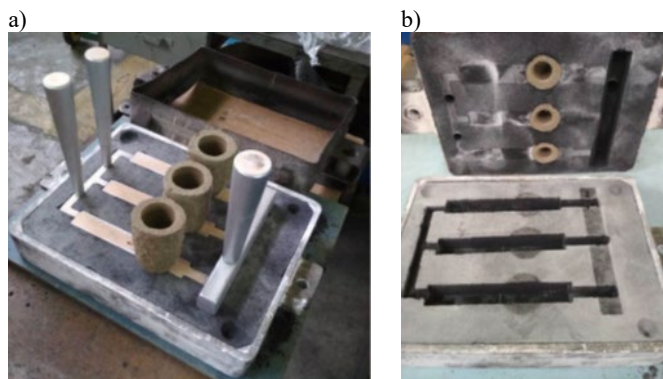
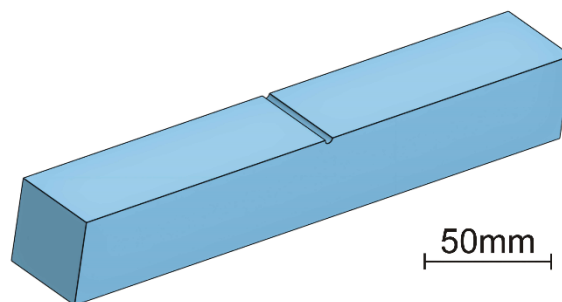


Fig. 3. View of a sample half-mould during moulding with a pattern set (a) and after pattern removal, before assembly of top and bottom parts (b)

a)



b)



Fig. 4. Scheme (a) and example view (b) of the impact test specimen according to PN-EN 15689

The adopted geometry of test castings followed the requirements of PN-EN 15689, which specifies the impact testing method obligatory for cast steel used in railway crossovers. The impact bending test consists of three successive dynamic loadings of a specimen supported at both ends by a free-falling hammer (mass: 50kg, drop height: 3m, striking edge radius: 50mm) (Fig. 5). The measure of impact resistance is the depth of the crack at the bottom of the U-notch, determined using a 5x optical device with 0,1mm accuracy (Fig. 6). According to PN-EN 15689, the impact resistance criterion is satisfied when the crack depth $U \leq 7,0\text{mm}$.

Hardness testing of the test castings was performed using the Brinell method with a 10mm tungsten carbide ball indenter, a 30kN load applied for 10s. For each variant, 12 measurements were taken. According to PN-EN 15689, the hardness criterion is satisfied when all measurements fall within 160÷260 HB and the hardness variation ΔHB is ≤ 50 HB.

It should be noted that in the scope of the mechanical properties, only impact resistance and hardness are required to assess the quality of crossover castings according to the obligatory standard PN-EN 15689.

Whereas the metallographic testing using a NIKON Eclipse LV150N (LOM) optical microscope and a scanning electron microscope Phenom ProX (SEM) with backscattered electron (BSE) imaging, electron beam accelerating voltage of 10 kV and with an energy X-ray dispersive spectrometer (EDS) were made. Metallographic specimens were etched in Nital of chemical

composition: with 5% nitric acid solution in ethanol.

3. Results and discussion

Figures 7÷10 show the microstructure of the studied manganese cast steel with varying Ni content after heat treatment, recorded using optical microscopy. At magnifications of 100x and 500x, it was found that the microstructure of samples with increased Ni content was fully austenitic after oversaturation. In contrast, “Ni-free” manganese cast steel (variant 0) exhibited an austenitic microstructure with individual (Fe, Mn) carbide precipitates after heat treatment, which resulted in higher hardness and lower impact resistance (Tab. 2, Fig. 11).

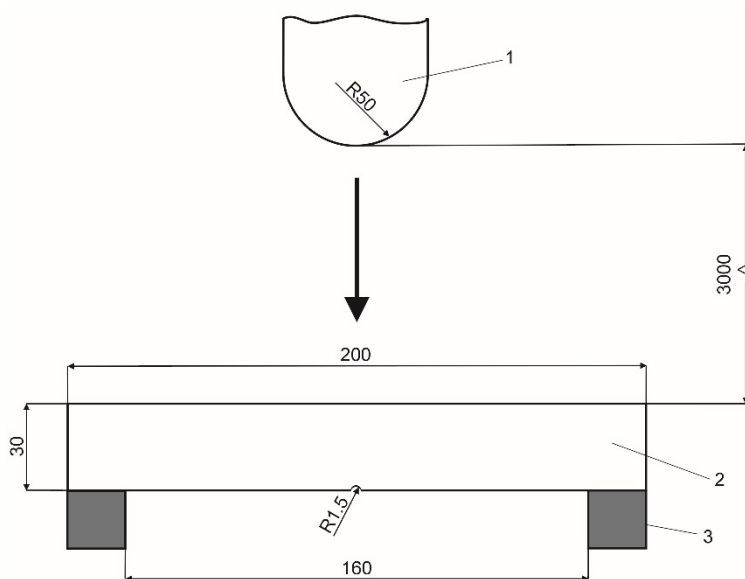


Fig. 5. Scheme of the impact bending test according to PN-EN 15689: 1 – hammer, 2 – sample and 3 - supports



Fig. 6. Specimen before (top) and after (bottom) impact bending test, showing the crack at the U-notch subjected to measurement

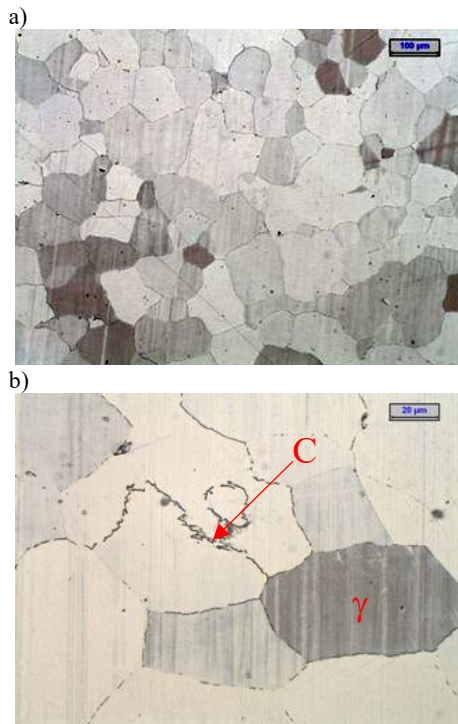


Fig. 7. Microstructure of manganese cast steel in an oversaturated state, variant 0, austenite (γ) and (Fe, Mn) carbides (C), etched: Nital, LOM: a) 100x, b) 500x

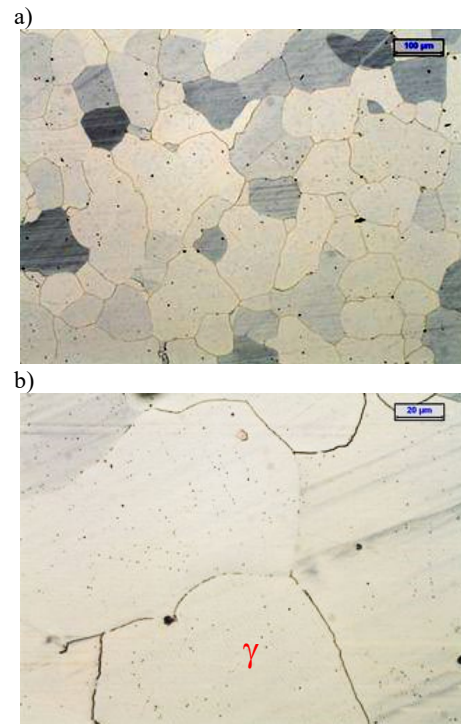


Fig. 9. Microstructure of manganese cast steel in an oversaturated state, variant 2, austenite (γ), etched: Nital, LOM: a) 100x, b) 500x

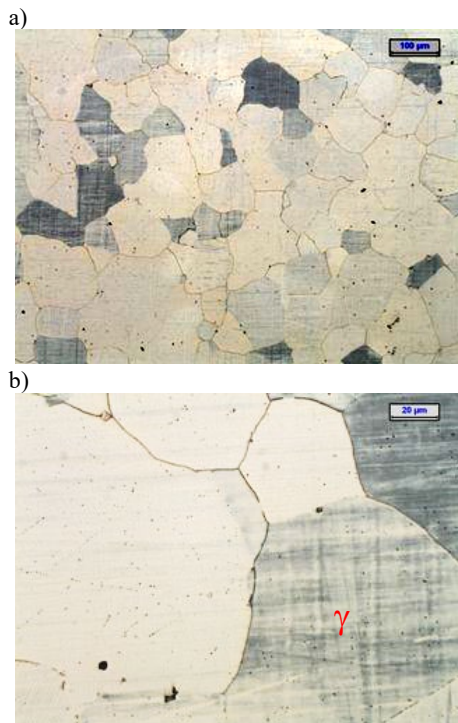


Fig. 8. Microstructure of manganese cast steel in an oversaturated state, variant 1, austenite (γ), etched: Nital, LOM: a) 100x, b) 500x

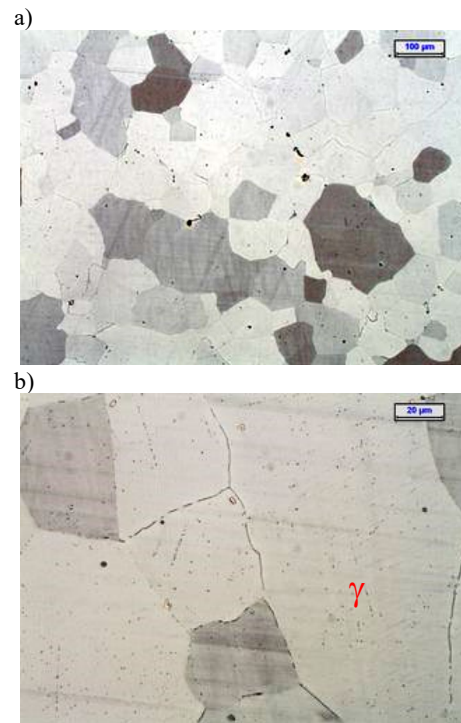


Fig. 10. Microstructure of manganese cast steel in an oversaturated state, variant 3, austenite (γ), etched: Nital, LOM: a) 100x, b) 500x

At higher magnifications in SEM observations (Figs. 12÷14), it was revealed that even in the austenitic microstructure of manganese cast steel in an oversaturated state with elevated Ni content, some alloy cementite ($(\text{Fe, Mn})_3\text{C}$) precipitates occurred at austenite grain boundaries. Their amount and distribution depended strongly on Ni content, generally decreasing as Ni concentration increased. In variant 1, alloy cementite formed a thin continuous network along austenite grain boundaries, which is unfavorable for impact resistance. In variant 2, carbides formed a thin discontinuous network, whereas in variant 3 they were absent, resulting in the highest impact resistance.

Therefore, it was found that both the hardness and impact resistance of manganese cast steel depend on the amount of hard ((Fe, Mn)) carbides present at the soft austenite grain boundaries. As the Ni concentration increases, the impact resistance and uniformity of hardness increase, initially by thinning the carbide network, then by disrupting its continuity, and finally by eliminating it. Exceeding the 1,0 wt.% of Ni concentration guarantees a significant improvement in impact resistance by approximately 40÷60% in comparison to the manganese cast steel

without Ni. While adding 0.5% Ni improves impact strength to a lesser extent, i.e. by approximately 25%.

In all examined variants, the presence of Ti carbonitrides was also identified (Figs. 15÷16). This phase is beneficial, since due to the crystal lattice similarity between $\text{Ti}(\text{C, N})$ and γ , it serves as an active base for heterogeneous nucleation of austenite, thus contributing to grain refinement. As a result of this refinement, the mechanical properties of the casting, particularly impact resistance, are improved. Therefore, inoculation of manganese cast steel with 0,05 wt.% Ti was confirmed as effective.

It was conclusively determined that, in order to achieve very high crack resistance of manganese cast steel intended for monoblock railway frogs, a Ni content of $\geq 1,0$ wt.% must be applied in combination with proper heat treatment of type oversaturation and inoculation with 0,05 wt.% of Ti. Use of the above-mentioned factors ensures hardness and impact resistance of manganese cast steel well exceeding the requirements of PN-EN 15689.

Table 2.

The results of hardness and impact resistance measurements of studied manganese cast steel in an oversaturated state

Variant		HB								$\overline{\text{HB}}^*$				ΔHB	U, mm				$\overline{\text{U}}$, mm**
0	217	217	207	207	207	207	217	241	217	229	217	229	218	34	4.7	4.9	4.5	4.7	
1	217	217	212	207	207	217	207	217	229	217	217	207	214	22	4.1	3.0	3.3	3.5	
2	207	212	217	207	212	212	217	217	207	207	207	207	211	10	2.5	2.7	2.8	2.7	
3	201	207	207	207	207	207	207	201	201	197	201	201	204	10	2.1	2.2	1.7	2.0	

* - HB standard deviation for variant 0 equals 10,1; for variant equals 1 is 6,6; for variant 2 equals 4,4 and for variant 3 equals 3,6.

** - U standard deviation for variant 0 equals 0,2; for variant equals 1 is 0,5; for variant 2 equals 0,1 and for variant 3 equals 0,2.

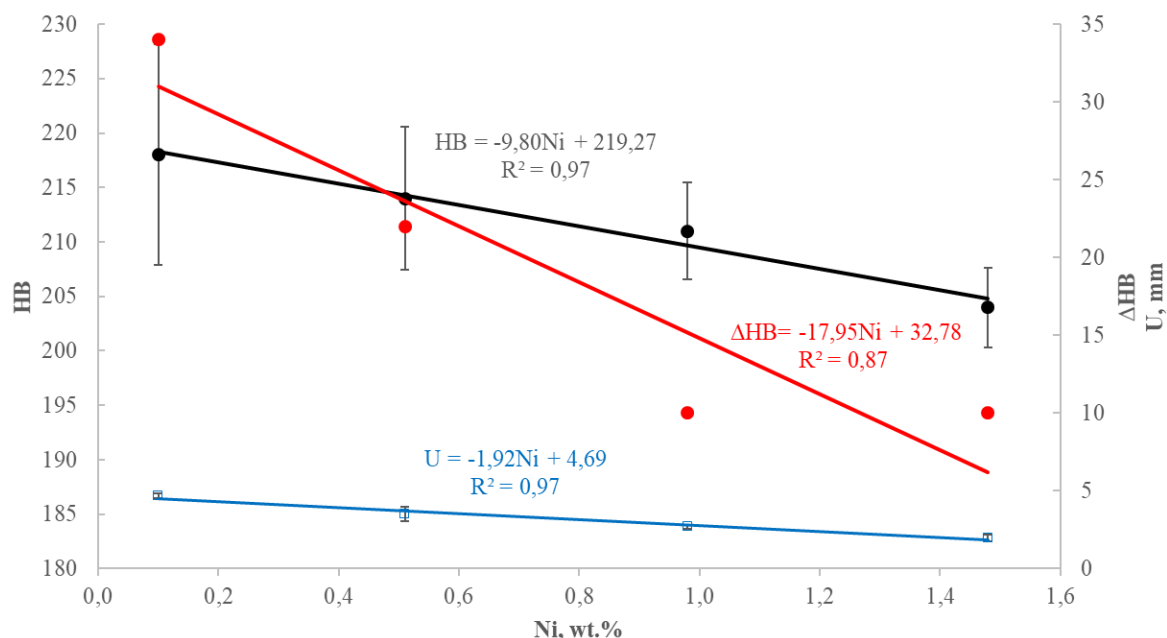


Fig. 11. Effect of Ni concentration on impact resistance U, hardness HB and its distribution ΔHB in the studied manganese cast steel in an oversaturated state

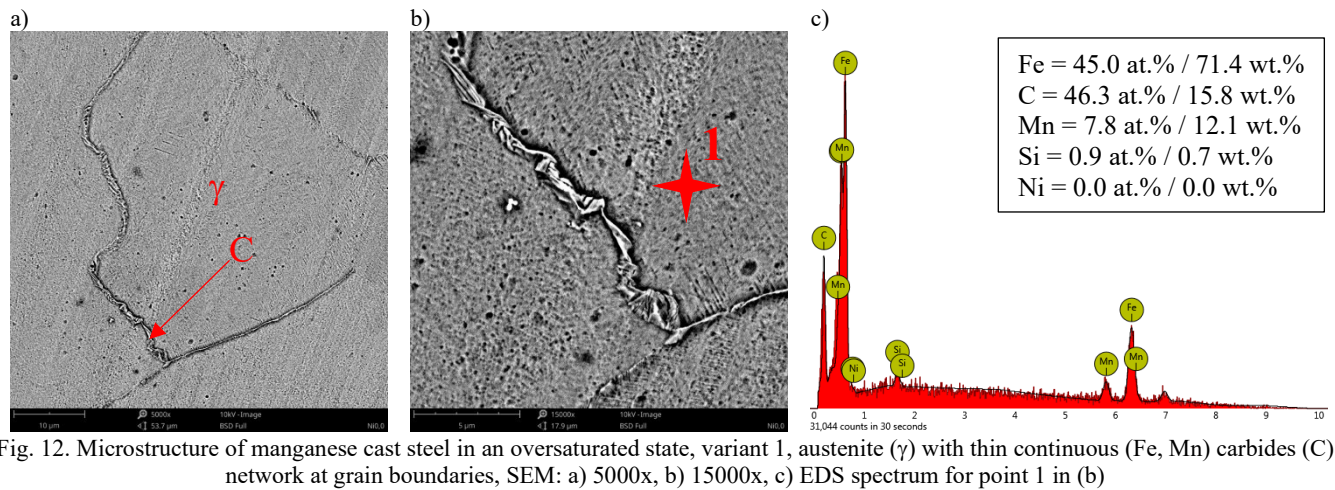


Fig. 12. Microstructure of manganese cast steel in an oversaturated state, variant 1, austenite (γ) with thin continuous (Fe, Mn) carbides (C) network at grain boundaries, SEM: a) 5000x, b) 15000x, c) EDS spectrum for point 1 in (b)

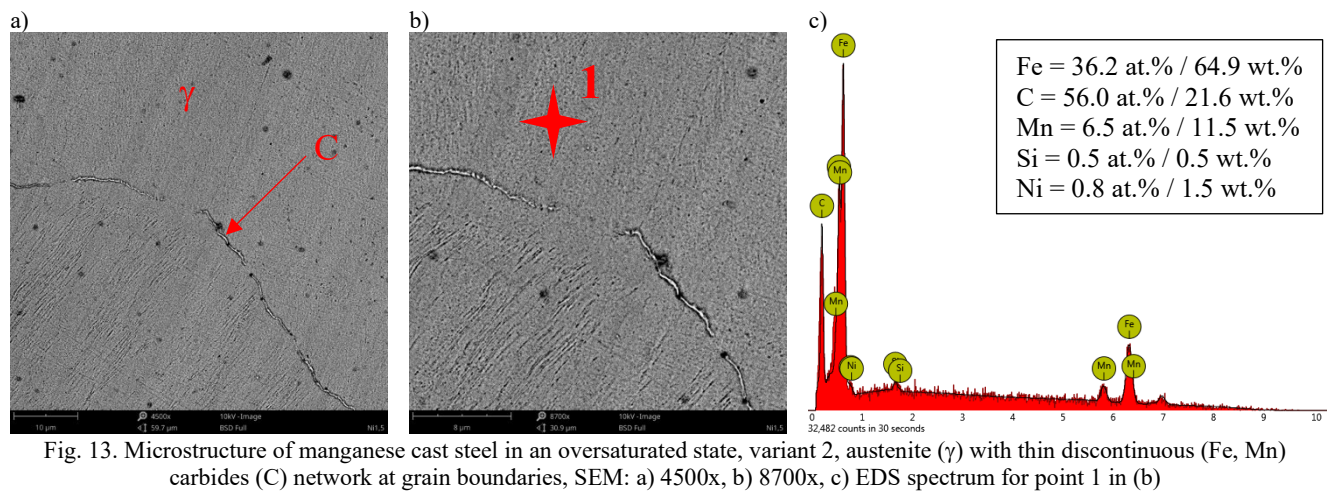


Fig. 13. Microstructure of manganese cast steel in an oversaturated state, variant 2, austenite (γ) with thin discontinuous (Fe, Mn) carbides (C) network at grain boundaries, SEM: a) 4500x, b) 8700x, c) EDS spectrum for point 1 in (b)

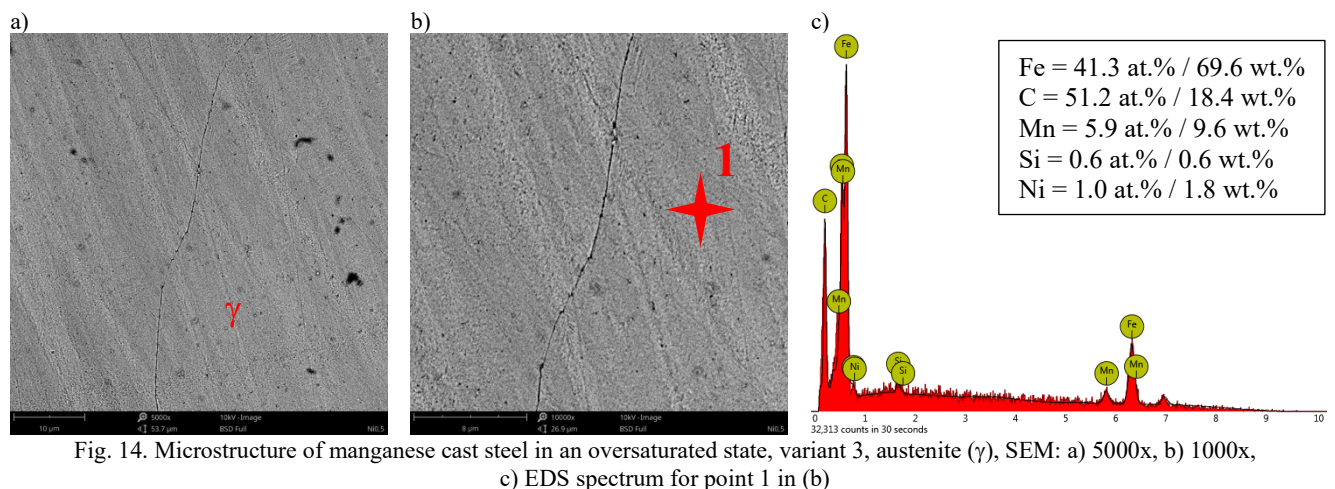


Fig. 14. Microstructure of manganese cast steel in an oversaturated state, variant 3, austenite (γ), SEM: a) 5000x, b) 10000x, c) EDS spectrum for point 1 in (b)

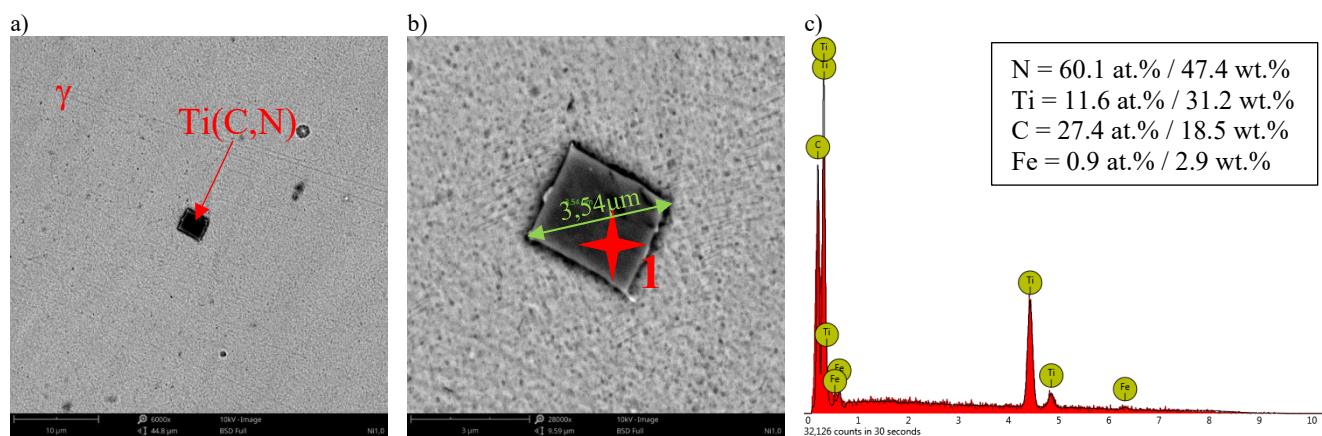


Fig. 15. Microstructure of manganese cast steel in an oversaturated state, variant 3, Ti(C,N) carbonitride in austenite (γ) matrix, SEM: a) 6000x, b) 28000x, c) EDS spectrum for point 1 in (b)

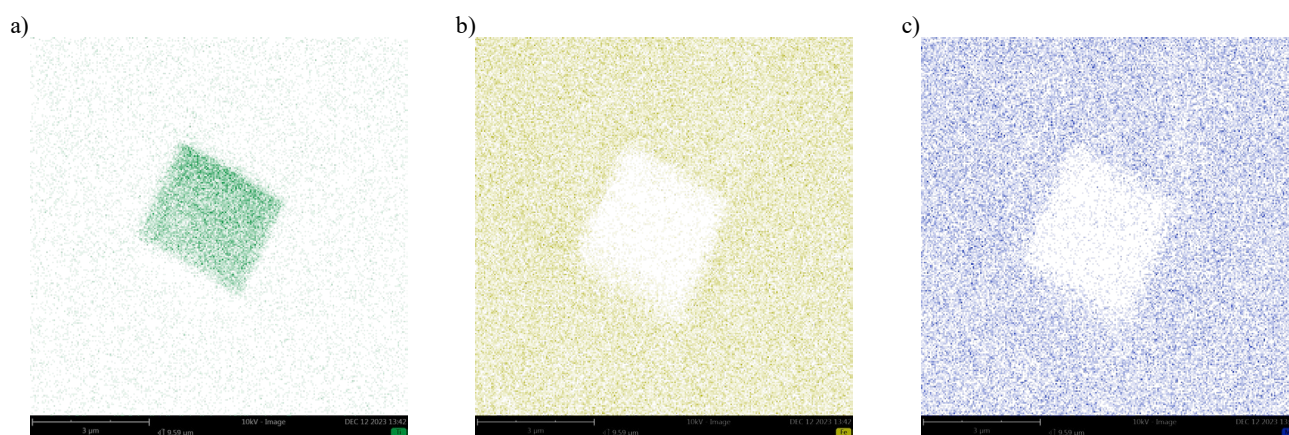


Fig. 16. Surface distribution of Ti (a), Fe (b) and Mn (c) in the area shown in Fig. 15b

4. Conclusions

Based on the analysis of the experimental results obtained, the following conclusions were formulated:

1. Variable Ni concentration in the range of approx. 0,1 to approx. 1,5 wt.% in manganese cast steel affects the phase composition of the microstructure and, consequently, the hardness and particularly the impact resistance of castings after heat treatment of type oversaturation.
2. Increasing Ni concentration in the studied manganese cast steel enhances impact resistance and homogenizes the hardness distribution of castings after heat treatment of type oversaturation.
3. Ni, as a strong austenite stabiliser, promotes the formation of a single-phase microstructure free of alloy cementite precipitates at austenite grain boundaries after oversaturation.
4. To obtain acceptable hardness while ensuring very high impact resistance, the chemical composition of manganese cast steel for railway crossovers should include an increased Ni concentration of ≥ 1 wt.%.

5. Modification of manganese cast steel with 0,05 wt.% Ti was positively evaluated, as Ti carbonitrides promote refinement of the austenitic microstructure, which is beneficial for the resulting mechanical properties of the casting.

Acknowledgements

The project was co-financed by the European Union from the European Regional Development Fund under the Intelligent Development Operational Program 2014-2020. The project is carried out as part of the competition of the National Center for Research and Development: Simple Fast Track.

References

- [1] Hadfield R.A. (1888). Hadfield's manganese steel. *Science*. 12, 284-286.

- [2] Petrov Y., Gavriljuk V., Berns H. & Schmalt F. (2006). Surface structure of stainless and Hadfield steel after impact wear. *Wear.* 260(6), 687-691. <https://doi.org/10.1016/j.wear.2005.04.009>.
- [3] Zhang G., Xing J. & Gao Y. (2006). Impact wear resistance of WC/Hadfield steel composite and its interfacial characteristic. *Wear.* 260(7-8), 728-734. <https://doi.org/10.1016/j.wear.2005.04.010>.
- [4] Atabaki M., Jafari S. & Abdollah-Pour H. (2012). Abrasive wear behavior of high chromium cast iron and Hadfield steel - a comparison. *Journal of Iron and Steel Research, International.* 19(4), 43-50. [https://doi.org/10.1016/S1006-706X\(12\)60086-7](https://doi.org/10.1016/S1006-706X(12)60086-7).
- [5] Kalandyk B., Tęcza G., Zapała R. & Sobula S. (2015). Cast high-manganese steel – the effect of microstructure on abrasive wear behaviour in Miller test. *Archives of Foundry Engineering.* 15(2), 35-38. DOI: 10.1515/afe-2015-0033.
- [6] Efsthathiou C. & Sehitoglu H. (2010). Strain hardening and heterogeneous deformation during twinning in Hadfield steel. *Acta Materialia.* 58(5), 1479-1488. <https://doi.org/10.1016/j.actamat.2009.10.054>.
- [7] Jabłońska M. (2016). *Structure and properties of a high-manganese austenitic steel strengthened in the result of mechanical twinning in processes of dynamic deformation.* Doctoral dissertation, Silesian University of Technology, Gliwice, Poland. (in Polish).
- [8] Głównia J. (2002). *Alloy steel castings – application.* Kraków: Fotobit. (in Polish).
- [9] Sobczak J. (2013). *Foundrymens handbook – Modern foundry engineering.* Kraków: STOP. (in Polish).
- [10] Aniołek K. & Herian J. (2013). Burdening and wearing railway switches in exploitation conditions and materials applied for their construction. *Eksploatacja.* 2-3, 85-89. (in Polish).
- [11] Havlíček P., Bušová K. (2012). Experience with explosive hardening of railway frogs from Hadfield steel. In Conference Proceedings of 21st International Conference on Metallurgy and Materials METAL, 23 – 25 May 2012 (pp. 705-711). Brno, Czech Republic.
- [12] Dhar S., Danielsen H., Fæster S., Rasmussen C., Zhang Y. & Jensen D. (2019). Crack formation within a Hadfield manganese steel crossing nose. *Wear.* 438-439, 203049, 1-9. <https://doi.org/10.1016/j.wear.2019.203049>.
- [13] Ma Y., Mashal A. & Markine V. (2018). Modelling and experimental validation of dynamic impact in 1:9 railway crossing panel. *Tribology International.* 118, 208-226. <https://doi.org/10.1016/j.triboint.2017.09.036>.
- [14] Wu T., Jeong H., Hsu W., Chang C. & Lai Y. (2024). Assessment of fatigue crack growth in metro cast manganese steel frogs and inspection strategy. *Engineering Failure Analysis.* 163(A), 108512, 1-15. <https://doi.org/10.1016/j.engfailanal.2024.108512>.
- [15] Zambrano O., Tressia G. & Souza R. (2020). Failure analysis of a crossing rail made of Hadfield steel after severe plastic deformation induced by wheel-rail interaction. *Engineering Failure Analysis.* 115, 104621, 1-24. <https://doi.org/10.1016/j.engfailanal.2020.104621>.
- [16] Machado P., Pereira J., Penagos J., Yonamine T. & Sinatora A. (2017). The effect of in-service work hardening and crystallographic orientation on the micro-scratch wear of Hadfield steel. *Wear.* 376-377(B), 1064-1073. <https://doi.org/10.1016/j.wear.2016.12.057>.
- [17] Harzallah R., Mouftiez A., Felder E., Hariri S. & Maujean J. (2010). Rolling contact fatigue of Hadfield steel X120Mn12. *Wear.* 269(9-10), 647-654. <https://doi.org/10.1016/j.wear.2010.07.001>.
- [18] Wróbel T., Jezierski J., Bartocha D., Feliks E. & Paleń A. (2024). Quality assessment method for chromite sand to reduce the number of cast steel surface defects. *Archives of Foundry Engineering.* 24(4), 31-38. <https://doi.org/10.24425/afe.2024.151307>.